Direct dynamical energy cascade in the modified KdV equation

Denys Dutykh, Elena Tobisch

Denys Dutykh
CNRS–LAMA, University of Savoie, France

Elena Tobisch
Johannes Kepler University, Linz, Austria

Direct dynamical energy cascade in the modified KdV equation

arXiv.org / HAL

DIRECT DYNAMICAL ENERGY CASCADE IN THE MODIFIED KDV EQUATION

DENYS DUTYKH AND ELENA TOBISCH*

Abstract. In this study we examine the energy transfer mechanism during the nonlinear stage of the Modulational Instability (MI) in the modified Korteweg–de Vries (mKdV) equation. The particularity of this study consists in considering the problem essentially in the Fourier space. A dynamical energy cascade model of this process originally proposed for the focusing NLS-type equations is transposed to the mKdV setting using the existing connections between the KdV-type and NLS-type equations. The main predictions of the D-cascade model are outlined and thoroughly discussed. Finally, the obtained theoretical results are validated by direct numerical simulations of the mKdV equation using the pseudo-spectral methods. A general good agreement is reported in this study. The nonlinear stages of the MI evolution are also investigated for the mKdV equation.

Key words and phrases: Modulational Instability; energy cascade; Korteweg–de Vries equation; modified KdV equation; NLS equation.

MSC: [2010]35Q53 (primary), 35Q55, 76E30 (secondary)

* Corresponding author.

Contents

1. Introduction

Nonlinear wave systems occur in numerous physical areas from optics to fluid mechanics, from astronomy to geophysics, and one of the most important issues regarding these systems is a description of its energy behavior. One of the most beautiful examples to illustrate this point, is the hypothesis of Kolmogorov on the form of energy spectrum in systems with strong turbulence, [29]. The theory describes the energy transfer from larger to smaller eddies – this is called a (direct) energy cascade, until the Reynolds number becomes small enough to stabilize the eddy's motion and viscosity begins to dissipate the kinetic energy. Under three main hypothesis, the energy spectrum is supposed to have the universal form $\mathcal{E}(\ell) \sim \ell^{-5/3}$ where ℓ is the size of the eddy. The main hypothesis are:

(1) existence of an energy conserving inertial range of space scales ℓ;
(2) in this range turbulence is locally homogeneous (no dependence on position);
(3) locally isotropic (no dependence on the direction).

This is an asymptotic theory and it works in the limit of very big Reynolds numbers, [13]. Experimental studies demonstrate very often a good agreement with this hypothesis but also contradictions, e.g. existence of an inverse energy cascade (from small to large eddies), appearance of large coherent structures at high Reynolds numbers, *etc.* Nowadays the theory of (strong) turbulence is further on developed and refined, [35].

The same three hypothesis, along with other assumptions, have been used in the kinetic wave (or weak) turbulence theory (WTT). Dispersive waves play now the role of eddies in the Kolmogorov's theory of turbulence, and the energy spectrum is computed as a stationary solution of the wave kinetic equation first introduced by Hasselmann in [20]. If dispersion function $\omega \sim k^{\beta}$, the form of energy spectra is again power law $k^{-\alpha}$ where k is the wave length first found by Zakharov & Filonenko (1971) for capillary water waves, [43]. However, the exponent α is not universal anymore, and its form depends on the dispersion function $\omega = \omega(k)$ as computed from the linear part of the corresponding weakly nonlinear dispersive evolutionary equation, [44]. If dispersion function has a more complicated form, e.g. $\omega^2 = gk + \sigma k^3$, no analytical predictions for the form of the energy spectra are given by the kinetic WTT.

This is also an asymptotic theory which is working for very small nonlinearity $0 < \varepsilon_{\text{kin}} \lessapprox 0.01$, where small parameter ε_{kin} is taken as a product of wave amplitude with wave number, $\varepsilon_{\text{kin}} = Ak$. The smallness of ε is very important while the kinetic WTT is essentially based on the following *assumption*: time scales for 3–, 4–, …, s–wave resonances are separated, at each time scale $t/\varepsilon_{\text{kin}}$, $t/\varepsilon_{\text{kin}}^2, \ldots$ different processes take place; these time scales are regarded independently. For the confirmation of the results of this theory, a lot of numerical simulations with the Euler equations and its reductions have been performed in which it was shown that theory breaks at about $\varepsilon \approx 0.1$, *e.g.* [2].

On the other hand, usual laboratory experiments and numerical simulations are performed for $\varepsilon \approx 0.1 \div 0.4$ for a very simple reason. For $\varepsilon \sim 0.01$ time scales $t/\varepsilon_{\text{kin}}$, $t/\varepsilon_{\text{kin}}^2, \ldots$

are too long and kinetic energy cascades (K-cascades) can not be observed in an experiment; examples of computations are given in [28]. Another questions and open problems in the kinetic WTT still awaiting their resolving can be found in [32].

A new model (hereafter referred to as D-model) for the formation of the energy spectrum has been developed by E. KARTASHOVA (2012) in [26]; the model can be applied for describing nonlinear wave systems with nonlinearity parameter of the order of $\varepsilon \sim 0.1 \div 0.4$ and wave systems with narrow frequency band excitation. Basic physical mechanism responsible for the formation of the energy spectrum in this model is not a s–wave resonance but the modulation instability, and the main assumption of the model is that energy cascade is formed by the most unstable modes in the system, *i.e.* modes with maximum increment of instability. In [26], the Increment Chain Equation Method (ICEM) for computing the energy spectrum of the D-cascade was developed for computing dynamical energy spectrum in the systems possessing modulation instability.

The ICEM has been applied for the focusing NLS and mNLS, and energy spectra for surface gravity and capillary waves were computed, with two different levels of nonlinearity. A comparison of time scales at which of the D-cascades and K-cascades occur is given in [28]. The form of the energy spectra in the D-model depends on the parameters of initial excitation and on the dispersion relation; the spectrum might have exponential decay, power law or even more complicated form as in the case of gravity-capillary waves, [37]. Various characteristic of a D-cascade pure gravity water waves — its direction, possible scenarios of cascade termination, *etc.* are described in [27].

The NLS is a very attractive equation because of its integrability, but unfortunately it gives sometimes not good enough description of the observed physical effects. WHITHAM (1967) [40] studied various situations where the use of the NLS equation can be justified or not in case of non-trivial three wave resonances. An example of non-trivial four wave resonances is given by the phenomenon of modulation instability was discovered in laboratory experiments and explained by BENJAMIN & FEIR (1967) [3], as instability of a narrow wave packet in the framework of the NLS. In particularly, the instability interval

$$0 \; < \; \Delta\omega \big/ Ak\omega \; \leq \; \sqrt{2}, \tag{1.1}$$

has been written out. Here $\omega(k)$ is the linear dispersion relation, k is the wavenumber and A is the amplitude of the Fourier mode ω. Quantity $\Delta\omega$ is the distance between the parent mode and its side band. The explicit analytical form of the instability interval is used for the construction of the D-cascade and will be discussed in the next Section.

However, numerical simulations with NLS demonstrate a symmetric energy cascade in the Fourier space while energy cascade experimentally observed in a water tank, is asymmetric. To cope with this problem, it is necessary to introduce various modifications to NLS, *e.g.* [9, 21]. These modification allow for the realistic values of small parameter, $0 < \varepsilon_{\text{real}} \sim 0.1 \div 0.4$, and is more suitable for modeling real physical phenomena.

Korteweg–de Vries (KdV) equation is another widely used model equation, especially for water waves, describing long wave limit, *i.e.* small wave vectors k. Though KdV does not have modulation instability [1], its various modifications do possess this property, under certain conditions. Thus, perturbations of a quasi-periodical wave train with small

amplitudes in the generalized KdV equations with nonlinearity of the form $(u^{p+1})_x$

$$\mathrm{gKdV}(u_\pm) \doteq u_t + u_{xxx} + (u^{p+1})_x = 0 \ , \tag{1.2}$$

are modulationally stable if $p < 2$, while they are modulationally unstable if $p > 2$, [19]. A more general version of this result allowing for nonlocal dispersion can be found in [23]. However, all these results does not allow nice analytical presentation for the instability interval as in (1.1), and a numerical study is unavoidable.

Our aim in this paper is to study a particular case with $p = 2$ and one space dimension — the so-called modified Korteweg–de Vries (mKdV) equation

$$\mathrm{mKdV}(u_\pm) \doteq u_t + u_{xxx} \pm 6u^2 u_x = 0 \ , \tag{1.3}$$

with u being a real-valued scalar function, x and t are space and time variables consequently, and the subscripts denote the corresponding partial derivatives.

As a starting point for our simulations aiming to study the MI in the mKdV, i.e. $p = 2$ in (1.2), we use the estimates obtained in [19] by combination of analytical results and numerical estimates, namely that for $p = 2$, the wave is spectrally stable for all wave vectors $0 < k^2 < 2$. Another reference point important for our study of mKdV is the following remarkable feature of this equation: it can be reduced, under certain conditions, to the mNLS where the MI can be studied by analytically. This reduction can be made by the variational methods [40] or by standard asymptotical approach as in [16].

It is also shown in [16] that wave packets are unstable only for a positive sign of the coefficient of the cubic nonlinear term in (1.3), and for a high carrier frequency. Being interested in modulation instability, we restrict the study further on the case of focusing mKdV equation:

$$\mathrm{mKdV}(u_+) \doteq u_t + u_{xxx} + 6u^2 u_x = 0. \tag{1.4}$$

In the present paper we aim to study formation and properties of D-cascade in the frame of KdV equation (1.4).

As there are several exact analytical solutions known for the (1.4) equation, we will use them for the verifying our numerical model. The exact cnoidal wave solutions to the KdV equation can be found in [6]:

$$u(x,t) = \frac{1}{\frac{s}{3s^2-1} + \frac{\sqrt{2(1-s^2)}}{6s^2-2}\sin\left(\sqrt{3s^2-1}(x-x_0-t)\right)} - s, \quad s \in \left[-1, -\frac{\sqrt{3}}{3}\right] \cup \left[\frac{\sqrt{3}}{3}, 1\right], \quad x_0 \in \mathbb{R}. \tag{1.5}$$

The one-soliton solution is given by

$$u(x,t) = a + \frac{b^2}{\sqrt{4a^2+b^2}\cosh y + 2a}, \quad y = bx - (6a^2 b + b^3)t + c \ , \tag{1.6}$$

where a, b, c are arbitrary constants, [31]. There exists also a rational solution of the form

$$u(x,t) = a - \frac{4a}{4a^2(x-6a^2t)^2 + 1} \ ,$$

where a is arbitrary constant, [33].

The present manuscript is organized as follows. In Section 2 we give a sketch of a D-cascade formation for this equation and formulate the properties of the cascade and its spectra which should be verified numerically. In Section 4 we describe shortly our numerical approach and present results of our numerical simulations. Finally, the main conclusions of this study are discussed in Section 5.

2. D-cascade in the model equation

Initially, the D-cascade has been introduced in the case of the NLS and mNLS equations [26]. The main mechanism generating this cascade is the side-band or modulational instability discovered first in optics in [4] and one year later in hydrodynamics [3].

It is well-known that the celebrated KdV equation does not possess the modulational instability. On the other hand, the mKdV equation does possess this property which is the object of our investigations. Moreover, it can be shown that the mKdV equation can be reduced to the well-studied mNLS case [16]. Consequently, our results apply in both cases.

The main effect of the Modulational Instability (MI) is the disintegration of periodic wavetrains in the deep water [42]. If we pick up a particular wave after a sufficiently long time evolution, we can assert that this wave is a result of the disintegration a parent wave into side bands. That is why the MI is also referred to in the literature as the side band instability.

Benjamin & Feir (1967) [3] showed that there is a connection between the frequencies, wavenumber and amplitudes of unstable modes in the framework of the focusing (+) Nonlinear Schrödinger (NLS) equation, which reads after a proper rescaling:

$$\mathrm{NLS}(v_{\pm}) \doteq \mathrm{i}v_t + v_{xx} \pm |v|^2 v = 0$$

Namely, they computed the instability interval in the form

$$0 \;<\; \Delta\omega \big/ Ak\omega \;\leq\; \sqrt{2}, \tag{2.1}$$

where $\omega(k)$ is the linear dispersion relation, k is the wavenumber and A is the amplitude of the Fourier mode ω. Quantity $\Delta\omega$ is the distance between the parent mode and its side band. Henceforth, the instability interval (2.1) contains the infinite number of unstable modes along with their potential side bands. It was conjectured that in the actual evolution of a physical system the selected side band leads to the most unstable solution which can be found by the computing of the so-called increment of instability (see the recent review by Zakharov & Ostrovsky (2009) [45] and the references therein). In the case of deep water waves Benjamin & Feir (1967) [3] showed that the most unstable mode satisfies the following relation:

$$\Delta\omega \big/ Ak\omega \;=\; 1. \tag{2.2}$$

Further on let us denote by (k_0, ω_0, A_0) the parameters set of the parent wave and $(k_{\pm1}, \omega_{\pm1}, A_{\pm1})$ will be used for the right and left side bands correspondingly. In these new variables we

can rewrite (2.2) as two separate equations for each side band frequency:

$$\omega_{\pm 1} \;=\; \omega_0 \;\pm\; A_0 k_0 \omega_0,$$

where $\varepsilon \doteq A_0 k_0$ is the wave steepness, which is assumed to be a small parameter hereinbelow. The side band amplitudes $A(\omega_{\pm 1})$ can be easily related to the parent mode amplitude in the following way:

$$A_{\pm 1} \;\doteq\; A\bigl(\omega_{\pm 1}\bigr) \;=\; A\bigl(\omega_0 \;\pm\; \varepsilon\omega_0\bigr).$$

The right-hand side can be expanded in the Taylor series

$$A_{\pm 1} \;=\; A\bigl(\omega_0 \pm A_0 k_0 \omega_0\bigr) \;=\; \sum_{s=0}^{+\infty} \frac{A_0^{(s)}}{s!} \bigl(\pm A_0 k_0 \omega_0\bigr)^s \;=$$

$$A_0 \;\pm\; A_0^{'} A_0 k_0 \omega_0 + \frac{1}{2} A_0^{''} \bigl(\pm A_0 k_0 \omega_0\bigr)^2 + \ldots \quad (2.3)$$

where the primes denote the differentiation with respect to ω_0. The expansion (2.3) is an explicit relation between the amplitudes of parent and side-band modes. This completes the first step of the D-cascade construction.

Let us assume that we already found the amplitudes of Fourier modes at the step $n-1$. The amplitudes $A_{\pm n}$ can be then constructed by applying recursively the same procedure (see Figure 1 for the illustration). Namely,

$$\omega_{\pm n} \;=\; \omega_{(n-1)} \;\pm\; \underbrace{A_{(n-1)} k_{(n-1)}}_{\varepsilon_n} \omega_{(n-1)}, \quad (2.4)$$

The last two relations are called the chain equations which constitute the basis of the D-cascade construction. A similar Taylor expansion yields

$$A_{\pm n} \;=\; A_{(n-1)} \;\pm\; A_{(n-1)}^{'} A_{(n-1)} k_{(n-1)} \omega_{(n-1)} + \frac{1}{2} A_{(n-1)}^{''} \bigl(\pm A_{(n-1)} k_{(n-1)} \omega_{(n-1)}\bigr)^2 + \ldots, \quad (2.5)$$

and the estimated in this way amplitudes $\{A_{\pm n}\}$ allow us to compute the energy spectra $\{|A_{\pm n}|^2\}$ in the Fourier space. The indices of positive (negative) sign correspond to the direct (inverse) energy cascade.

Equation (2.5) could be considered as an Ordinary Differential Equation (ODE) with respect to the one unknown wave amplitude $A_{(n-1)}(\omega_0)$, if we knew the wave amplitude $A_{\pm n}(\omega_0)$ at the next recurrence step. This infinite system of equations can be closed if we assume that at some level of this hierarchy we know the relation between $A_{\pm n}$ and $A_{\pm(n-1)}$. It turns out that in recent experiments on the capillary wave turbulence [41] it was shown that it is the simplest functional relation (*i.e.* proportionality) which is realized:

$$A_{\pm n} \propto A_{\pm(n-1)} \quad \Rightarrow \quad A_{\pm n} \;=\; \sqrt{p} A_{\pm(n-1)}, \quad 0 \;<\; p \;<\; 1.$$

By keeping only the first two terms in the Taylor expansion (2.5) and using the last closure relation we obtain

$$\sqrt{p} A_n \;\approx\; A_n \pm A_n^{'} A_n k_n \omega_n \quad \Rightarrow \quad A_n^{'} \;=\; \pm \frac{\sqrt{p} - 1}{\omega_n k_n},$$

where ω_0, A_0 are excitation parameters, n is the common index and $p = p(\omega_0, A_0)$. The last ODE can be solved in quadratures

$$A(\omega_{\pm n}) \;=\; \pm(\sqrt{p}-1)\int_{\omega_0}^{\omega_{+n}} \frac{\mathrm{d}\omega_n}{\omega_n k_n} \;+\; C_{\pm}(\omega_0, A_0, p) \tag{2.6}$$

Accordingly, by definition the energy $E_n(\omega_n) \propto A^2(\omega_n)$, which provides us with the discrete set of energies of individual harmonics. The spectral density $\mathcal{E}^{(\mathrm{Dir})}(\omega)$ can be now computed

$$\mathcal{E}^{(\mathrm{Dir})}(\omega) \doteq \lim_{\Delta\omega_n \to 0} \frac{E(\omega_{n+1}) - E(\omega_n)}{\Delta\omega_n}.$$

A similar formula can be written for the inverse cascade as well. However, the limits of integration in (2.6) will be inverted correspondingly to $\int_{\omega_{-n}}^{\omega_0}$.

2.1. Geometrical interpretation

In this section we would like to provide a simple geometrical interpretation of the energy cascade formation described hereinabove. On Figure 1 we illustrate the first three steps of the direct cascade (towards increasing frequencies) according to the chain rule (2.4). The cascading modes are shown with vertical solid lines. On the other hand, the non-cascading (or broadening) modes are depicted with dashed lines. Since at every step of the cascade there is a formation of two modes, only one being cascading, we observe the fast spectrum broadening. This process is schematically shown in Figure 2 where cascading and non-cascading modes are shown as colored and empty circles correspondingly. Modes with bigger amplitudes are shown with bigger circles. A simple combinatorial computation shows that after n cascade steps 2^n Fourier modes will be excited at most. Finally, on Figure 3 we show the fully developed Fourier spectrum formed as a result of the D-cascade formation.

2.2. Assumptions of the D-cascade model

In this Section we summarize the main hypotheses behind the D-cascade model.

The main assumption about the initial state consists in the narrow frequency banded excitation, in contrast to previous cascade models proposed by Kolmogorov (strong turbulence) and Zakharov (weak turbulence) which require the excitation of the whole Fourier spectrum (all scales). However, most practical situations fall into the class of problems with rather a narrow forcing.

The main mechanisms driving the energy cascade is the Modulational Instability (MI). That is why the nonlinearity parameter is bounded from above by the physical wave breaking limitation which depends on a system in hand. For water wave problem $\varepsilon_{\mathrm{MI}} \lessapprox 0.1 \div 0.4$. On the other hand, our approach does not have the limitation on the time scales when the cascading process takes place. In the kinetic theory the K-cascade occurs on the time scale $t \;\propto\; \varepsilon^{2(2-s}$, where s is the minimal number of waves which interact resonantly (with a non-vanishing interaction coefficient), while in the D-cascade the time scale is independent of generic resonances.

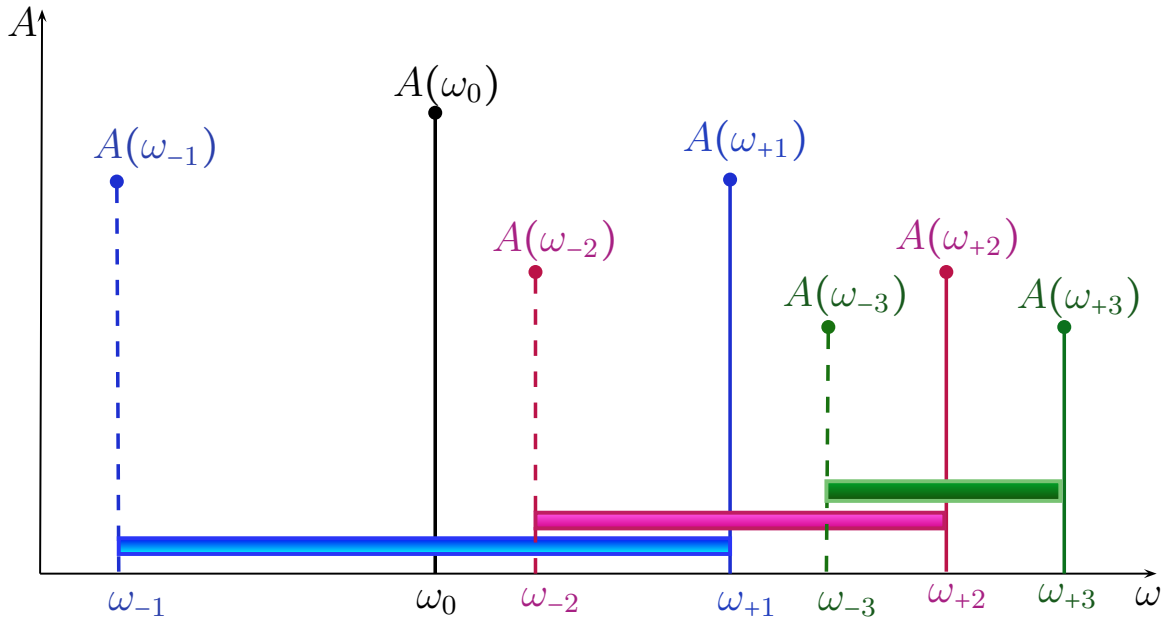

Figure 1. *Schematic representation of the initial stage of the direct cascade formation. The pairs of modes created at the same step of the cascade are shown with the same color and connected with a horizontal bar.*

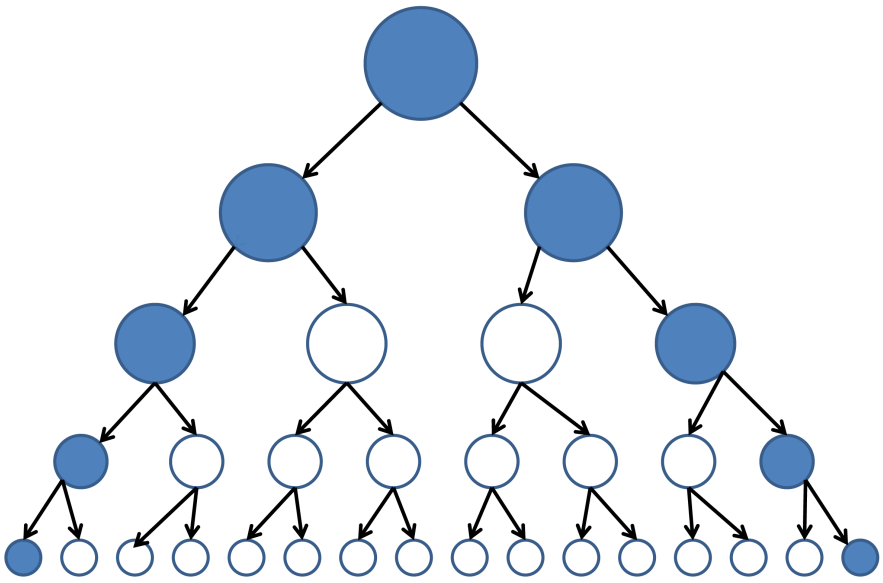

Figure 2. *Schematic representation of the cascade broadening. Cascading modes are shown as blue circles, non-cascading (or broadening) modes — as empty circles. The relative circle size indicates the energy content of the mode.*

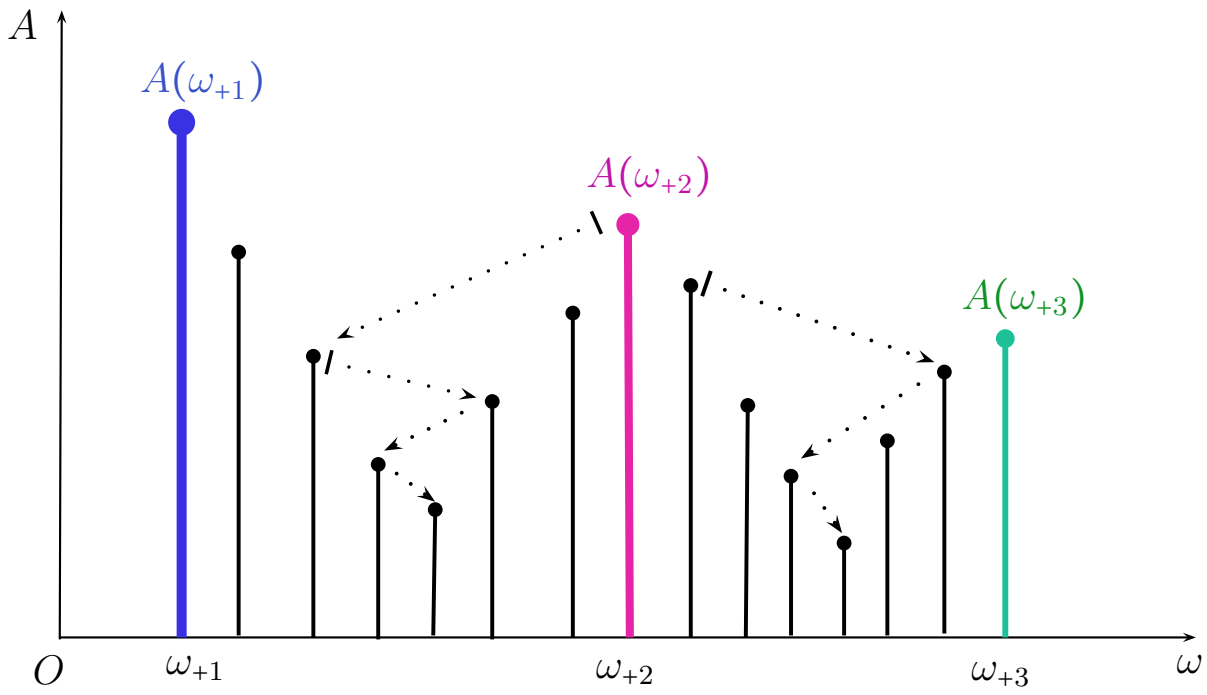

Figure 3. *Illustration to the final stage of the cascade stabilization due to the spectrum broadening.*

Finally, another technical assumption states that the cascade is formed of the most modulationally unstable modes.

2.3. Predictions of the D-cascade model

The main predictions of the D-cascade model are summarized below.

Directly, from the definition of the MI (as a special case of 4–wave interaction) it follows that it occurs on the time scale $t_{\mathrm{MI}} \propto t/\varepsilon^2$. Additionally, from the chain equations (2.4) it follows that the distance between the frequencies dependes on the initial wave steepness (or another nonlinearity problem parameter).

One can easily see from the chain equations (2.4) that the frequency $\omega_{\pm n}$ depends nonlinearly on the previous frequency $\omega_{(n-1)}$ and amplitude $A_{(n-1)}$. Moreover, after simple calculations one can show that the chain equations at every step correspond to the exact resonance of four 2 nd order Stokes waves [37]. Consequently, the assumption of the modulational instability can be replaced by another assumption of the existence of exact Stokes wave resonance. It broadens somehow the applicability of the model, while the MI remains a very useful setting to describe the D-cascade.

The model allows to compute approximatively the Fourier spectrum shape. Strictly speaking its form will also depend on the problem degree of the nonlinearity ε and the initial conditions (A_0, ω_0). For small nonlinearities a satisfactory description can be provided by a family of NLS equations written in the vicinity of every cascading mode. For moderate

nonlinearities one needs to take into account the higher order effects which result in the mNLS-type terms. In general, the spectrum decays exponentially. At the cascade step n the energy is $\mathcal{E}_n \propto p^n \mathcal{E}_0$ where $\mathcal{E}_0$ is the energy of the initially excited mode $\mathcal{E}_0 = |A_0|^2$ and p is the cascade intensity. In various laboratory experiments (*e.g.* [41]) it was observed that the cascade intensity p can be assumed and to be constant with high degree of accuracy. Then, the estimation of p from the measured data becomes straightforward. For the theoretical investigations the cascade intensity p can be explicitly written out as a function of the excitation A_0 and ω_0 for a given dispersion relation $\omega = \omega(k)$:

$$p = p\big(A_0, \omega_0, k_0\big),$$

where the functional dependence is different for every wave system under consideration.

The direction (*direct* or *inverse*) of the cascade can be determined from the recurrence relation for the cascading wave frequencies (2.4):

Direct: if $\omega_n > \omega_{n-1}$
Inverse: otherwise

Once the energy spectrum has been determined, this condition can be checked by the direct substitution for the expression for A_n. For example, for the direct cascade one obtains:

$$\omega_{\pm n} - \omega_{n-1} = \pm A_{n-1} k_{n-1} \omega_{n-1} = \Big(\pm(\sqrt{p} - 1) \int_{\omega_0}^{\omega_{\text{st}}} \frac{\mathrm{d}\omega_n}{\omega_n k_n} + C_{\pm}(\omega_0, A_0, p)\Big) k_{n-1}\omega_{n-1} > 0.$$

The last inequality provides us with a sufficient condition for the direct cascade formation. It is straightforward to obtain a similar condition for the inverse cascade by changing the limits of integration and inequality sign to the opposite. Moreover, it was also observed that once the direction is determined, it will remain true for all $n > 0$.

A special attention has to be payed when $\omega_{\pm n} - \omega_{n-1} \approx 0$, but $\omega_{\pm n} - \omega_{n-1} \neq 0$ (the equality to zero is a condition of the cascade termination, see the next Section). In this case the appearance of both direct and inverse cascades is possible. Moreover, this situation was observed experimentally for surface water waves in [39].

From the D-cascade construction we can see that several scenarios of its termination are possible. The cascade termination is another strong prediction of the model described above. Some most probable scenarios are described in more details below in Section 2.4. Moreover, in Section 2.5 we demonstrate how this D-cascade model can be applied to the 4^{th} order NLS equation to compute energy spectra of capillary waves.

2.4. Cascade termination in the Fourier space

Since every Stokes wave is unstable, one could think that the cascading process will continue indefinitely. However, it is not necessarily the case, unless a very special initial condition is chosen[1]. In this section we will describe several most probable *scenarios* of the ending of the cascade process. However, this list is not exhaustive. See [27] for more information.

[1] This class of initial conditions for surface gravity waves was described in [27].

2.4.1 Stabilization process

The cascading process is terminated when the instability condition (2.1) is not fulfilled. At this step the chainrule (2.4) breaks as well and no further modes can be generated. This situation is referred to as the *stabilization process*. From (2.4) one can obtain the following termination condition $\omega_{\pm n} = \omega_{\pm(n-1)} \equiv \omega_{\rm st}$, *i.e.*

$$\omega_{\pm n} - \omega_{n-1} \;=\; \pm A_{n-1} k_{n-1} \omega_{n-1} = \Big(\pm(\sqrt{p}-1) \int_{\omega_0}^{\omega_{\rm st}} \frac{{\rm d}\omega_n}{\omega_n k_n} \;+\; C_{\pm}(\omega_0, A_0, p)\Big) k_{n-1}\omega_{n-1} = 0.$$

After substituting the linear dispersion relation $\omega(k)$ into the last equation, one obtains an implicit relation for k_{n-1} and the initial parameters of the problem which provides the cascade stabilization in the Fourier space at frequency $\omega_{\rm st}$. In particular, for dispersion relations of the type $\omega \propto k^{\alpha}$ (with $\alpha \neq 1$) this condition will become an algebraic equation. For gravity waves in deep water this condition was studied in [27].

2.4.2 Wave breaking mechanism

The cascade is triggered from one Fourier harmonics with the nonlinearity $Ak \equiv \varepsilon_0$ given by the initial conditions. In the course of the cascade development the number of cascading modes grows linearly. If all cascading modes are considered as a single wave packet, its steepness $\varepsilon_{\rm wp}$ will be equal to

$$\varepsilon_{\rm wp} \;=\; \varepsilon_0 \;+\; \varepsilon_1 \;+\; \varepsilon_2 \;+\; \ldots$$

If the total steepness of the wavepacket $\varepsilon_{\rm wp} \geqslant \varepsilon_{\rm cr}$, where $\varepsilon_{\rm cr}$ is the limiting Stokes wave steepness, the wave breaking will inevitably occur. This mechanism was confirmed in laboratory experiments [8].

2.4.3 Intermittency mechanism

We remind that the modulational instability is a 4-wave resonance process of a very special kind. Namely, the interacting modes have very close frequencies along with wavenumbers. During the cascade evolution many other Fourier harmonics become excited and some generic 4–wave or even 3–wave resonances are possible. The intensity of these interactions depends on the interaction coefficient. It may happen that such interaction involves both a cascading and a non-cascading mode with the intensity stronger than the MI. In this case, the energy, instead of following the cascade direction, will enter in such quasi-periodic resonant interactions with non-cascading modes. This will be the sign of the intermittency. This scenario was observed experimentally in [39].

To make a conclusion, the choice of the stabilization scenario which will occur depends on the excitation parameter and the initial condition.

2.5. Example of the energy spectrum computation

For the sake of illustration, we will obtain the energy spectra for the pure capillary waves where $\omega(k) \propto k^{-3/2}$. Hogan (1985) [21] derived for this case a fourth-order modified

Nonlinear Schrödinger (mNLS) equation in (2+1)d which reads:

$$\mathrm{mNLS}(v) \doteq 2\mathrm{i}v_t + \tfrac{3}{4}v_{xx} + \tfrac{3}{2}v_{yy} + \tfrac{1}{8}|v|^2 v = -\tfrac{3}{4}\mathrm{i}v_{xyy} - \tfrac{1}{8}\mathrm{i}v_{xxx} - \tfrac{1}{16}\mathrm{i}v^2 v_x^\star + \tfrac{3}{8}\mathrm{i}|v|^2 v_x + v\bar{\phi}_x,$$

where $v(x,t)$ is the envelope of the free surface elevation and $\bar{\phi}$ is the mean flow potential (see [21] for more details).

Under the conditions of the small nonlinearity, the maximum instability condition reads [21]:

$$\frac{\Delta\omega_n}{\frac{1}{24}A_n k_n \omega_n} = 1.$$

All computations are completely similar to the examples presented above. The ODE equation to determine the wave amplitudes become

$$\pm(\sqrt{p}-1)A_n \approx \frac{1}{24}A_n'\omega_n^{5/3}.$$

Then, the direct and inverse discrete energy spectra can be readily obtained:

$$E^{(\mathrm{Dir})}(\omega_n) \propto \left[\frac{(1-\sqrt{p})}{16}\omega_n^{-2/3} + C^{(\mathrm{Dir})}\right]^2, \quad E^{(\mathrm{Inv})}(\omega_n) \propto \left[-\frac{(1-\sqrt{p})}{16}\omega_n^{-2/3} + C^{(Inv)}\right]^2,$$

$$C^{(\mathrm{Dir})} \doteq A_0 - \frac{(1-\sqrt{p})}{16}\omega_0^{-2/3}, \quad C^{(\mathrm{Inv})} \doteq A_0 + \frac{(1-\sqrt{p})}{16}\omega_0^{-2/3}.$$

Accordingly, the energy densities for these both cases read

$$\mathcal{E}^{(\mathrm{Dir})}(\omega) \propto -\frac{(1-\sqrt{p})^2}{16}\omega^{-7/3} - C^{(\mathrm{Dir})}(1-\sqrt{p})\omega^{-5/3},$$

$$\mathcal{E}^{(\mathrm{Inv})}(\omega) \propto -\frac{(1-\sqrt{p})^2}{16}\omega^{-7/3} + C^{(\mathrm{Inv})}(1-\sqrt{p})\omega^{-5/3}.$$

3. MI in the mKdV equation

The following generalized Korteweg–de Vries (gKdV) equation was derived by R. Grimshaw (2002) [15] as a weakly nonlinear model for internal long waves in a stratified fluid. After some transformations of the variables, the gKdV equation can be written in unscaled variables:

$$\mathrm{gKdV}: v_t + vv_x + v^2 v_x + v_{xxx} = 0$$

A simple change of variables given in [16] allows to reduce the last gKdV equation to the mKdV equation (1.3) with positive nonlinearity:

$$u_t + u_{xxx} + 6u^2 u_x = 0,$$

where $u = v + \frac{1}{2}$, $x \mapsto x + \frac{1}{2}t$. Let us remind that the mKdV equation is integrable and it can be reduced to the KdV equation through the Miura transformation which is briefly explained in Appendix A. By following Grimshaw *et al.* (2001) [16] the mKdV equation can be also reduced to the NLS equation describing the dynamics of weakly nonlinear wave packets [34]. Let us seek for a solution in the form

$$u(x,t) = \varepsilon A_1(X,T)\mathrm{e}^{\mathrm{i}\theta} + \varepsilon^2 A_2(X,T)\mathrm{e}^{2\mathrm{i}\theta} + \text{c.c.} + \ldots,$$

where $\theta \doteq kx - \omega t$, $\omega \doteq -k^3$, $X \doteq \varepsilon X$, $T \doteq \varepsilon t$ and $\varepsilon \ll 1$ is a small parameter. By $A_{1,2}(X,T)$ we denote the first and the second harmonics correspondingly. Substituting this solution ansatz into the mKdV equation, one obtains a hierarchy of asymtotic relations. For the first harmonic we obtain:

$$\varepsilon^2\Big(\frac{\partial A_1}{\partial T} + c_g\frac{\partial A_1}{\partial X}\Big) + \varepsilon^3\Big(\mathrm{i}k\frac{\partial^2 A_1}{\partial X^2} + 6\mathrm{i}k|A_1|^2A_1\Big) = \mathcal{O}(\varepsilon^4),$$

where $c_g = -3k^2 \doteq \dfrac{\partial\omega}{\partial k}$ is the group velocity of the carrier wave. After making the Galilean transform $\xi \doteq X - c_gT$ and $\tau \doteq \varepsilon T$ and droping the index 1, the last equation becomes the classical Nonlinear Schrödinger (NLS) equation to an asymptotic accuracy $\mathcal{O}(\varepsilon^4)$:

$$\mathrm{i}\frac{\partial A}{\partial \tau} = 3k\frac{\partial^2 A}{\partial \xi^2} + 6k|A|^2A. \tag{3.1}$$

By derivation equation (3.1) describes the envelope propagation for the mKdV solutions. Since both models are modulationally unstable, the D-cascade model can be applied to them. However, the NLS equation is built upon the additional assumption of the narrow band spectrum. Consequently, the D-cascade for a single NLS equation consists of only one cascading mode, possibly accompanied with the spectrum broadening. This situation is illustrated on Figure 4 where equation (3.1) was solved numerically for a modulated plane wave initial condition.

The full description of a non-trivial cascade in the NLS framework requires a sequence of the NLS models: each NLS equation describing the vicinity of a cascading mode. On the other hand, the mKdV equation does not have such restrictions. Consequently, we can expect to observe the full D-cascade in this model.

4. Numerical simulations

In order to solve numerically the KdV equation on a periodic domain we used the classical Fourier-type pseudo-spectral method [5, 38]. The derivatives are computed in the Fourier space, while the nonlinear products – in the physical one (with the linear CPU-time). Thanks to the FFT algorithm [11, 10, 12] the passage between these two representations is done in the super-linear time $\mathcal{O}(N\log(N))$, which determines the overall algorithm complexity (per time step). For the dealiasing we used the classical 2/3-rule [38] which was combined (when necessary) with the Fourier smoothing method proposed in [22] for more delicate treatment of higher frequencies. The discretization in time was done with the embedded adaptive 5^{th} order Cash–Karp Runge–Kutta scheme [7] with the adaptive PI step size control [18].

Since our main goal in this paper is a comparison of the theoretical predictions of the D-cascade model against the numerical solutions to the focusing mKdV equation (1.4), the numerical solver was validated first on the simple tests of the cnoidal wave propagation (see Figure 5, $s = 0.75$) and the overtaking collision of solitary waves (see Figure 6). We checked that up to the numerical accuracy the spectrum was stationary in the former simulation showing that the wave is perfectly preserved by the numerical solver and no

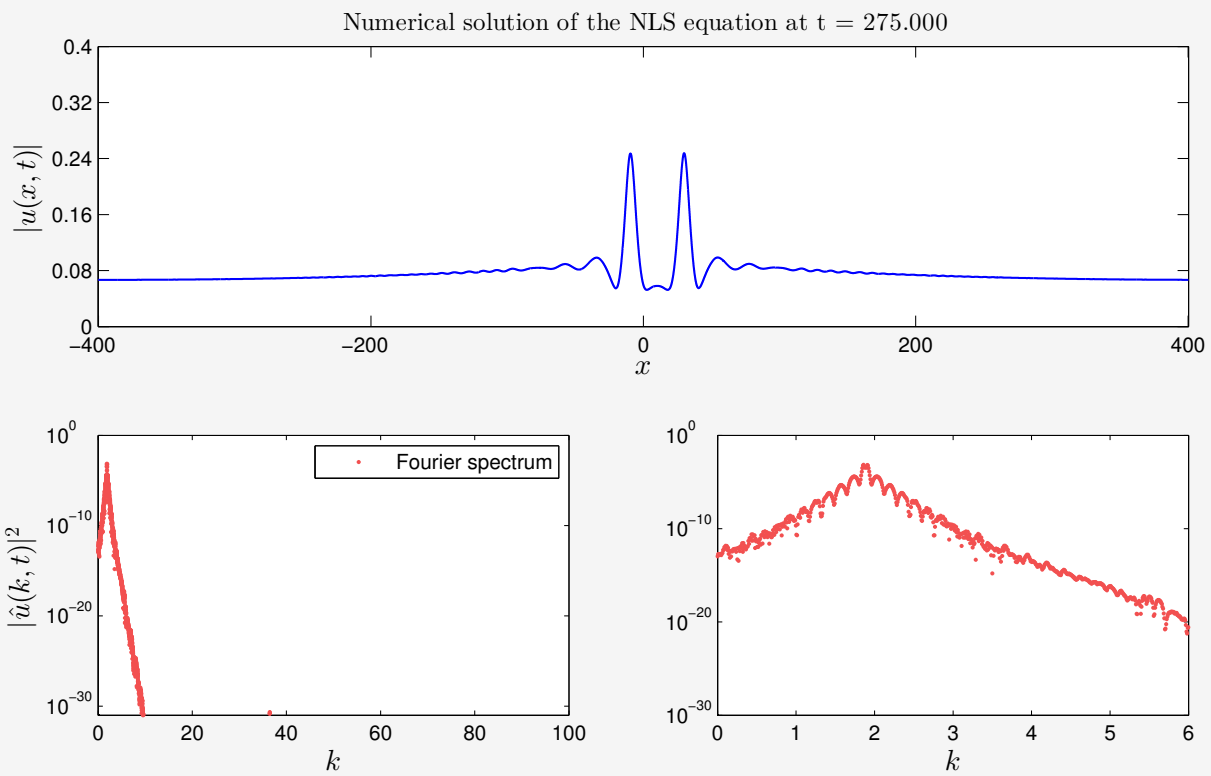

Figure 4. *MI in the NLS equation* (3.1) *for the initial condition parameters given in Table 1.*

dispersive tail was present after the collision in the latter, confirming the integrability of the mKdV equation.

For our numerical simulations of the Modulational Instability (MI) we adopt the set-up used also earlier in [17]. We consider the following initial condition posed on a periodic domain $[-\ell, \ell] = \left[-\pi/k_0, \pi/k_0\right]$:

$$u(x,0) \equiv u_0(x) = a\big(1 + \delta \sin(K_0 x)\big) \sin(k_0 x), \tag{4.1}$$

where a is the base wave amplitude, δ is the perturbation magnitude and the wavenumbers k_0, K_0 are chosen such that their ratio $k_0/K_0 \in \mathbb{Z}$. The values of parameters are given in the Table 1. The number N of Fourier modes used in simulations presented below will be set to $N = 32768$ and the tolerance parameter in the PI step size control was set to 10^{-8}.

4.1. Effect of the spectral domain

For the Fourier domain limited to $k \in [0,\ 8]$ the simulation results shown on Figures 7 and 8 are in a good qualitative agreement with the results presented in [17]. Unfortunately the authors in [17] did not report the evolution of the Fourier spectrum. We will fill in this gap in the present study. For instance, one can notice the presence of a second peak in the Fourier spectrum (in the vicinity of $k \approx 6$) which corresponds to the second cascading

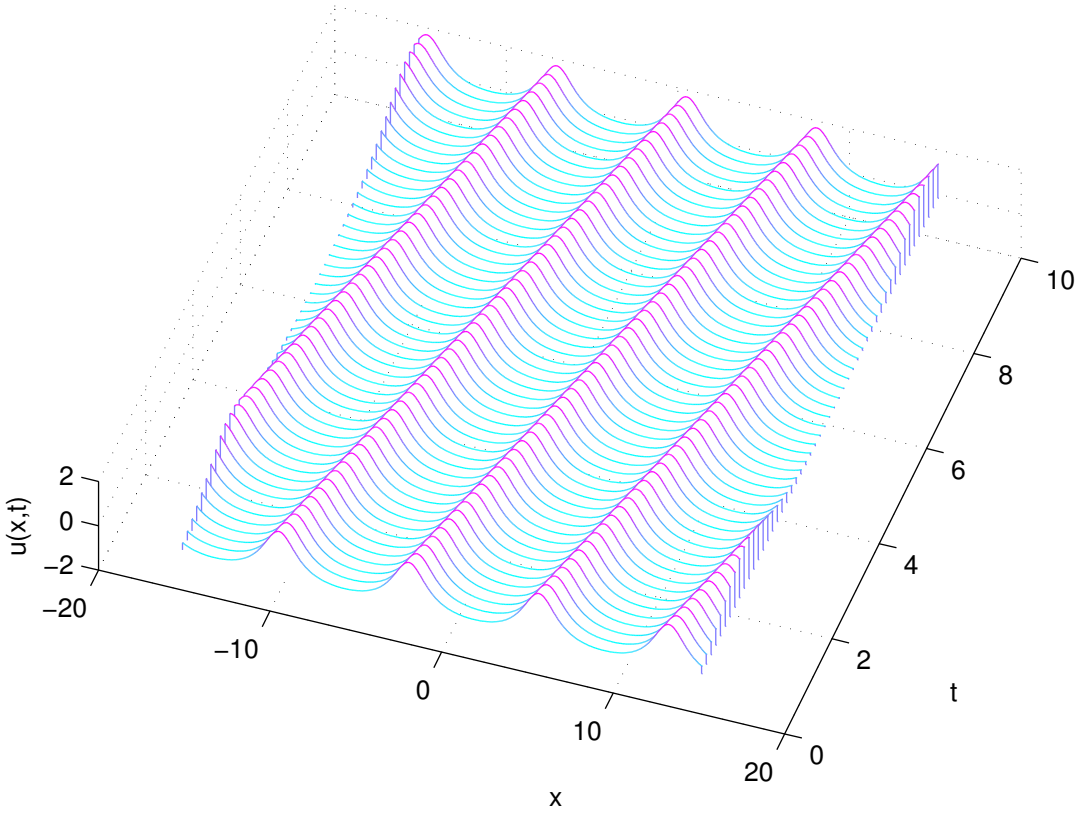

Figure 5. *Free propagation of a cnoidal wave in the mKdV equation for the parameter* $s = 0.75$.

Base wave amplitude, a	0.08
Perturbation magnitude, δ	0.05
Base wavenumber, k_0	1.884
Perturbation wavenumber, K_0	0.00785
Ratio of wavelengths, k_0/K_0	240

Table 1. *Numerical parameters from the previous study [17] used for the comparison with the present results.*

mode. During the development of the MI we observe a broadening of the spectrum around two cascading modes present in this numerical simulation. This broadening continues until the MI is fully developed (see Figure 8(*c, d*)). The left and right broadening wings can appear to be symmetric up to the graphical resolution, however our measurements reported in Table 2 show that it is not actually the case. The broadening intensities defined as the ratio of energies of two consecutive modes, *i.e.* $\beta_{\mathrm{r,l}} \doteq \frac{|u_{k\pm1}|^2}{|u_k|^2}$ and observed in the experiments depend on the initial wave amplitude. Namely, when the nonlinearity is

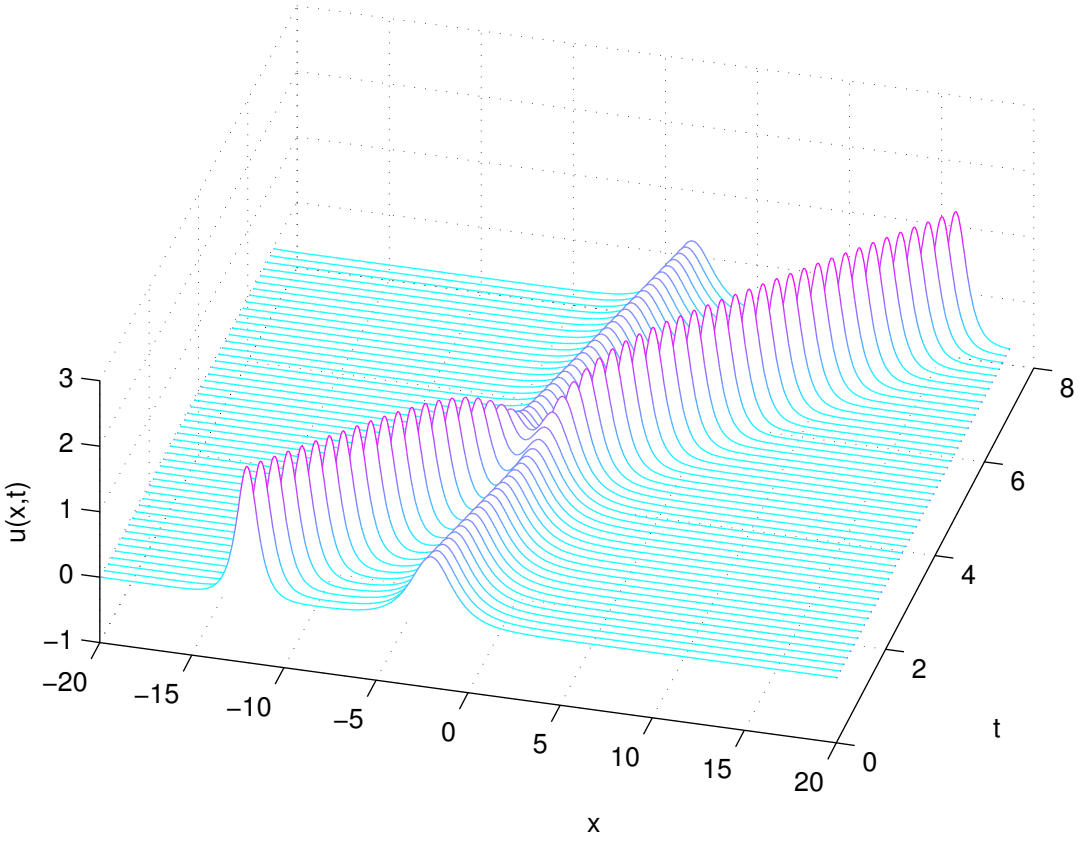

Figure 6. *Overtaking solitons collision in the mKdV equation.*

Amplitude, a	*Left intensity*, β_l	*Right intensity*, β_r
0.02	2.109	2.085
0.03	1.590	1.550
0.04	1.406	1.367
0.05	1.340	1.314
0.08	1.292	1.253

Table 2. *The left and right spectrum broadening intensities measured in numerical simulations of the mKdV equation for different values of the base wave amplitude. The measurements were made at the fully developed MI.*

increased, the broadening tails become flatter, thus involving more Fourier harmonics into this process.

In order to observe more than two cascading modes, the Fourier space has to be broaden. These results are shown on the left panel of Figure 9. In this case the Fourier domain is almost four times larger going up to $k = 32$. Accordingly to the theoretical predictions, the direct D-cascade is formed from the first instances of the numerical simulation. The

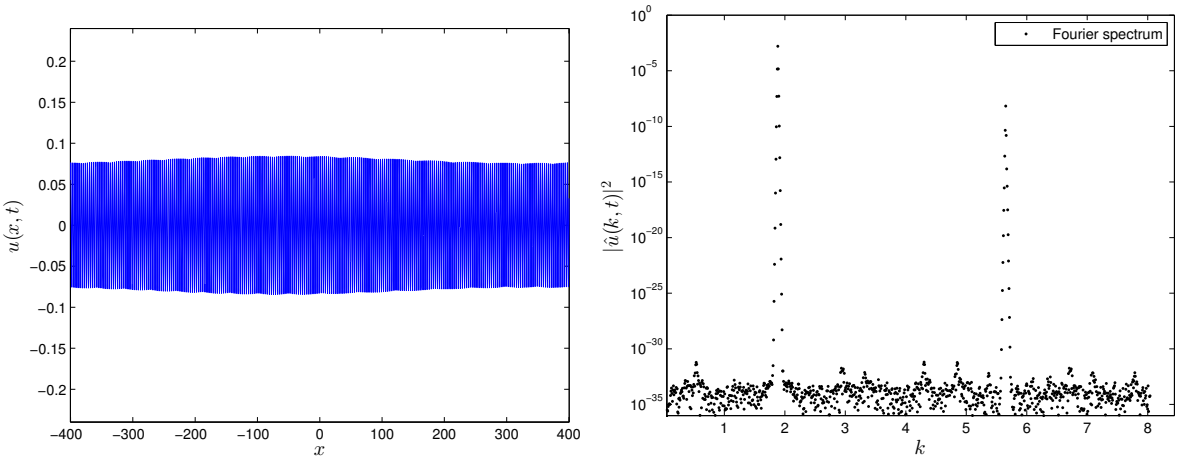

(a) Solution at $t = 100.0$ (b) Fourier spectrum at $t = 100.0$

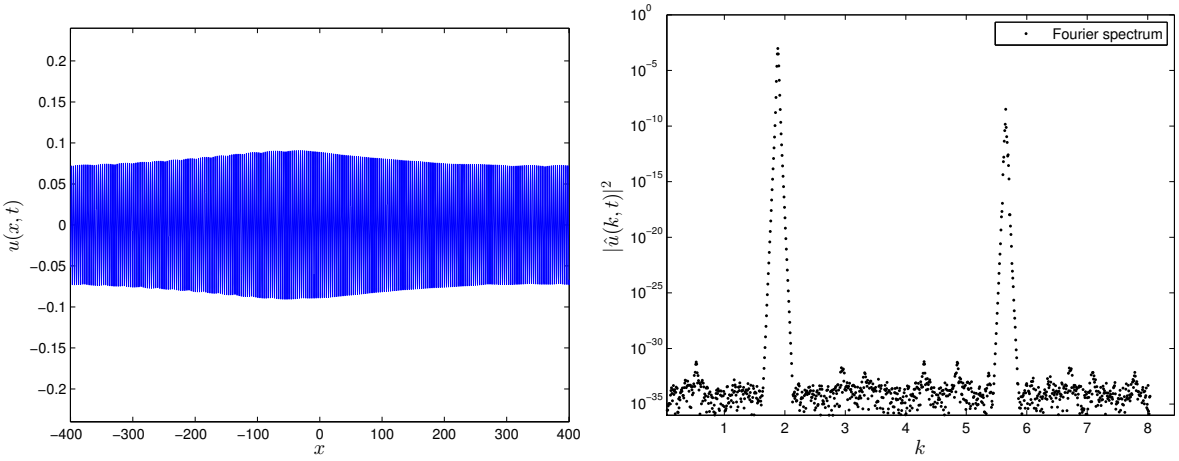

(c) Solution at $t = 400.0$ (d) Fourier spectrum at $t = 400.0$

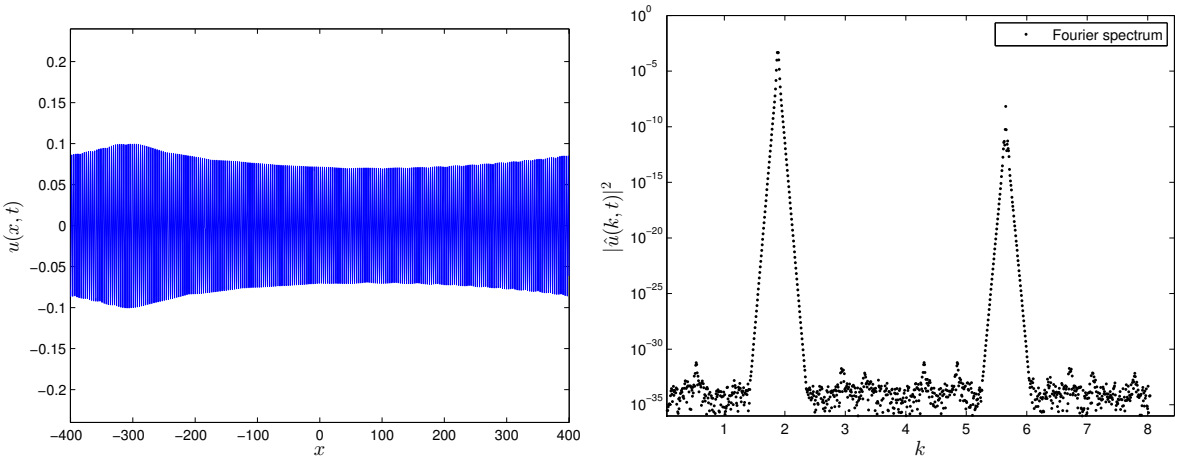

(e) Solution at $t = 510.0$ (f) Fourier spectrum at $t = 510.0$

Figure 7. *Development of the modulational instability in the mKdV equation for parameters given in Table 1. The left panel shows the mKdV solution and on the right panel we show the Fourier spectrum for* $k \in [0,\ 8]$.

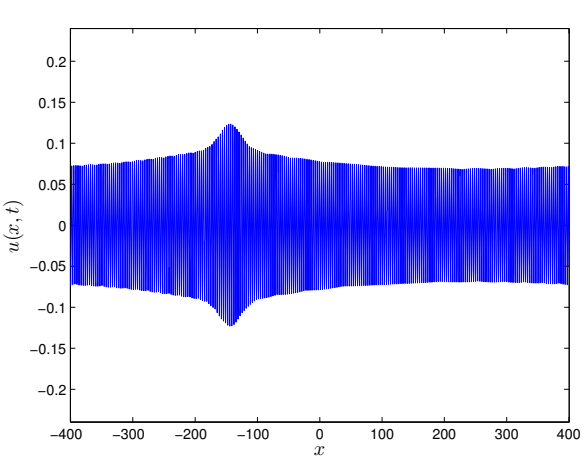

(a) Solution at $t = 560.0$

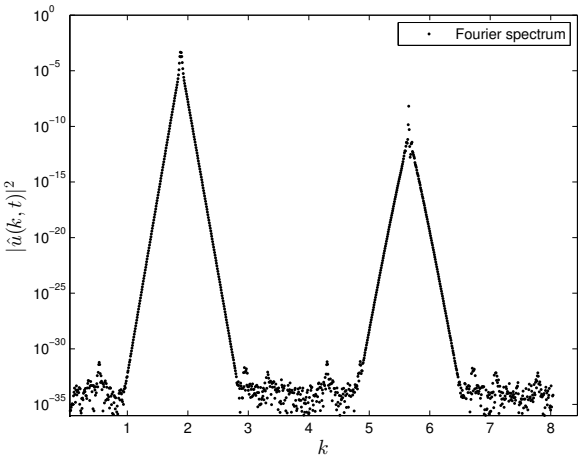

(b) Fourier spectrum at $t = 560.0$

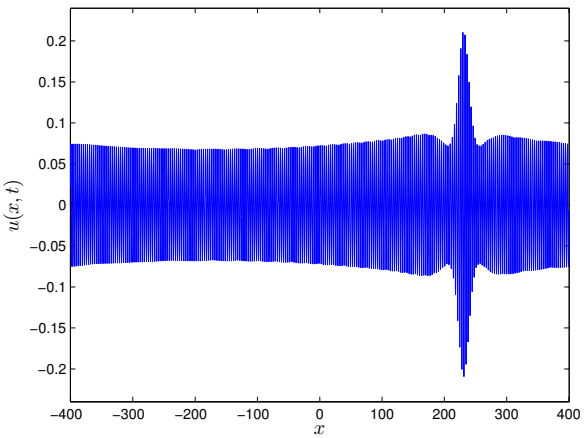

(c) Solution at $t = 600.0$

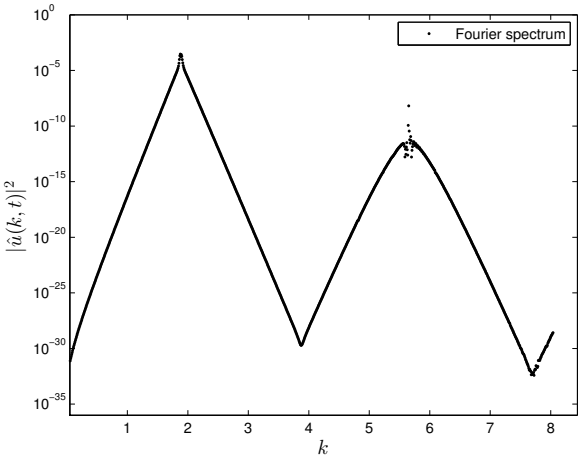

(d) Fourier spectrum at $t = 600.0$

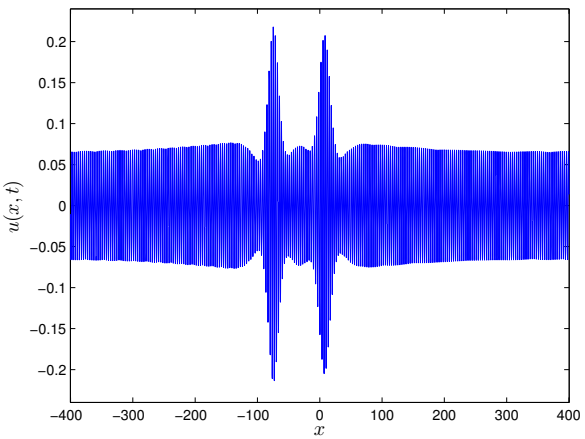

(e) Solution at $t = 700.0$

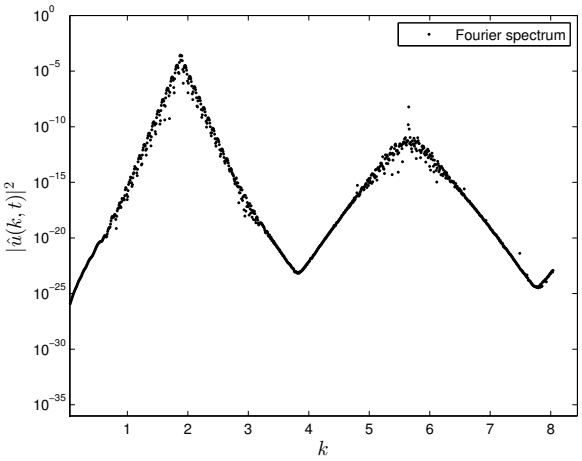

(f) Fourier spectrum at $t = 700.0$

Figure 8. *(Continued). See Figure 7 for the detailed description.*

linear fit in the Fourier space suggests the exponential shape of the energy spectrum $\mathcal{E}_k \propto \exp(-\alpha k)$, for some positive value of the slope α. Moreover, we computed the distances between two successive cascading modes. It turns out that this value is constant to the numerical precision (obviously, for a fixed initial condition).

4.2. Effect of the excitation amplitude

In this Section we study the effect of the base wave amplitude on the development of the MI in the mKdV equation. Namely, we perform the same simulation described in the previous section with numerical parameters given in Table 1, except for the amplitude a which will be chosen as $2a = 0.16$ and $3a = 0.24$. Moreover, we will take a larger spectral domain $k \in [0, 32]$ in contrast to the previous case. A larger domain is precisely needed to observe several cascading modes and to make some conclusions on their distribution in the Fourier domain. The simulation results are shown on Figures 9 and 10.

In particular, one can see that the initial condition with the amplitude two times bigger ($a = 0.16$) develops the MI much faster. According to the theoretical predictions [28], the time T_{MI} needed for the MI to be fully developed in the physical space scales as $T_{\mathrm{MI}} \propto \mathcal{O}(\varepsilon^{-2})$. So, the increase of the amplitude leads also to the increase in the nonlinearity ε. Consequently, our numerical results corroborate this prediction of the theory. On the other hand, we stress that the position (and consequently the distance between) of the cascading modes remains unaffected by the change in the amplitude.

4.3. Effect of the excitation wavenumber

On Figures 9 and 10 the base wavenumber k_0 was fixed and taken from Table 1. In this Section we describe the numerical experiments for another value of the parameter $k_0 = 5 \times 1.884$. The results of numerical simulations are reported on Figures 11 and 12. Namely, on Figure 11 it is shown that the new exponent of the spectrum is much lower than in the previous case. Moreover, if we increase the base wave amplitude a for the new value of $k_0 = 9.42$, the spectrum shape remains constant, however we cannot affirm anymore that it is still exponential as it is hinted on Figure 12. The positions and energies of cascading modes for these two simulations are reported in Table 3. From these observation one can clearly see that the initial wave amplitude does not affect the structure of the D-cascade.

Another important consequence of the variation of the parameter k_0 is the distance between cascading modes in the Fourier space. More precisely, the distance increases with the increase in k_0. For example, our simulations show that the distance increases from $\Delta k \approx 3.81$ to 18.42 when k_0 goes from 1.884 to $5 \times 1.884 = 9.42$.

4.4. Effect of the perturbation magnitude

In the numerical simulations performed so far we have always taken the perturbation with magnitude $m = 0.05$, which results in 5% amplitude modulation in terms of the base

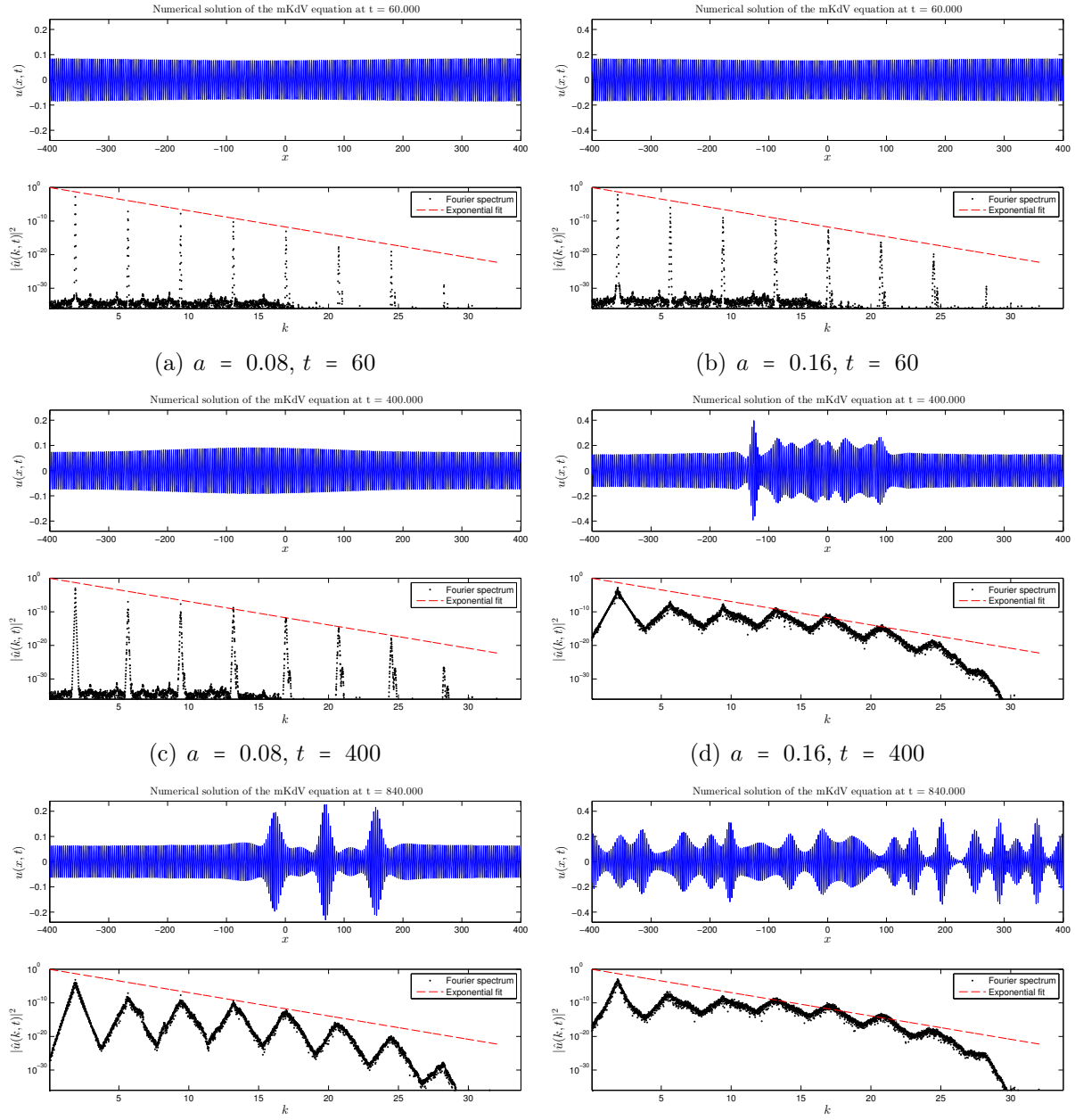

(a) $a = 0.08$, $t = 60$ (b) $a = 0.16$, $t = 60$

(c) $a = 0.08$, $t = 400$ (d) $a = 0.16$, $t = 400$

(e) $a = 0.08$, $t = 840$ (f) $a = 0.16$, $t = 840$

Figure 9. *Development of the MI in the mKdV equation for the initial wave amplitudes* $a = 0.08$ *(left panel) and* $2a = 0.16$ *(right panel) and several simulation times.*

wave amplitude a. We tested various values of parameter m in our numerical tests. Here we report on Figure 13 the most severe case of $m = 0.5$ (*i.e.* 50% of the perturbation). Even in such an extreme case, the D-cascade is still present. However, we cannot state

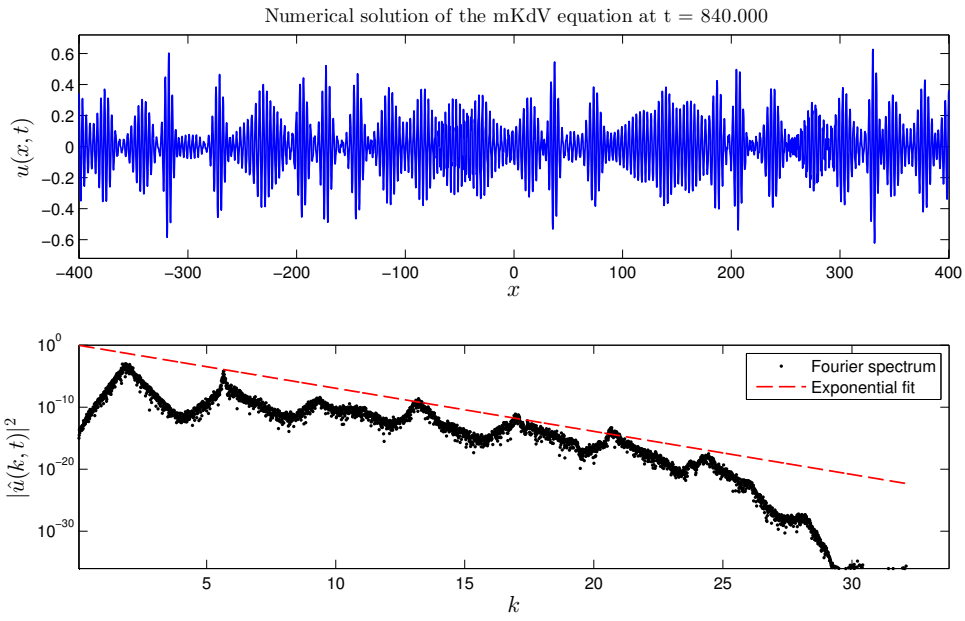

Figure 10. *Development of the MI in the mKdV equation for the initial wave amplitude* $3a = 0.24$ *at the final simulation time* $T = 840$.

a	0.08					
k	9.428	28.26	47.11	65.94	84.8	103.6
$\mathcal{E}$	3.35×10^{-4}	2.83×10^{-5}	5.07×10^{-6}	6.35×10^{-7}	5.29×10^{-10}	1.79×10^{-13}
a	0.16					
k	9.396	28.27	47.09	65.92	84.77	103.6
$\mathcal{E}$	1.04×10^{-3}	4.30×10^{-5}	1.18×10^{-5}	8.15×10^{-8}	3.52×10^{-10}	3.2×10^{-14}

Table 3. *Wavenumbers and energies of cascading modes for* $a = 0.08$ *and* $a = 0.16$. *The simulation snapshots are shown on Figure 12(a,b) correspondingly.*

anymore with certitude that its shape is exponential. This questions will require more detailed investigations with even more resolved numerical simulations.

5. Discussion

In this study we have investigated the D-cascade formation in the framework of the mKdV equation. The main mechanism generating this cascade is the Modulational Instability (MI). Since the D-cascade is not a widely known model yet, we reproduced its construction. Moreover, in the earlier publications it was described only for the NLS-type equations, while the main focus here is on the mKdV equation (1.3). A geometrical interpretation was provided along with the NLS equation derivation from the mKdV.

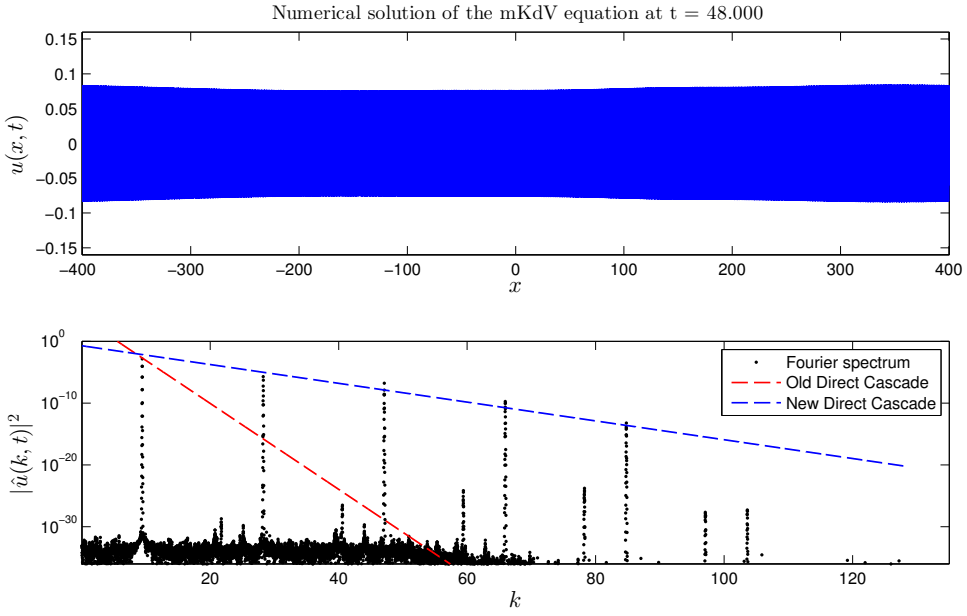

(a) $t = 48$

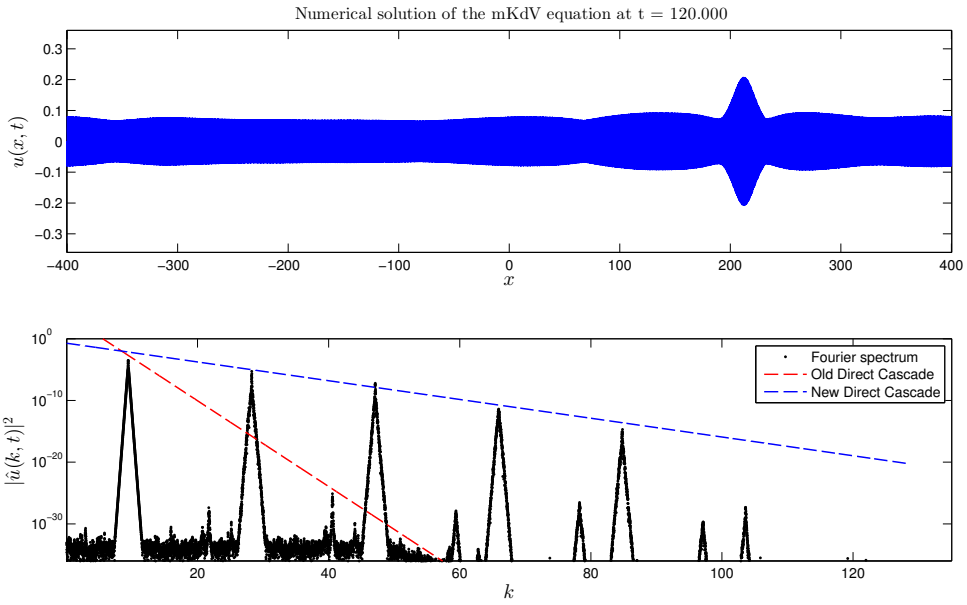

(b) $t = 150$

Figure 11. *MI simulation for* $k_0 = 5 \times 1.884$*, all the other parameters are the same as given in Table 1. The red dashed line on the bottom panels indicates the fit of the previous simulations for* $k_0 = 1.884$*. The blue dashed line shows the new fit. The magenta dashed line shows the direction of the eventual inverse cascade.*

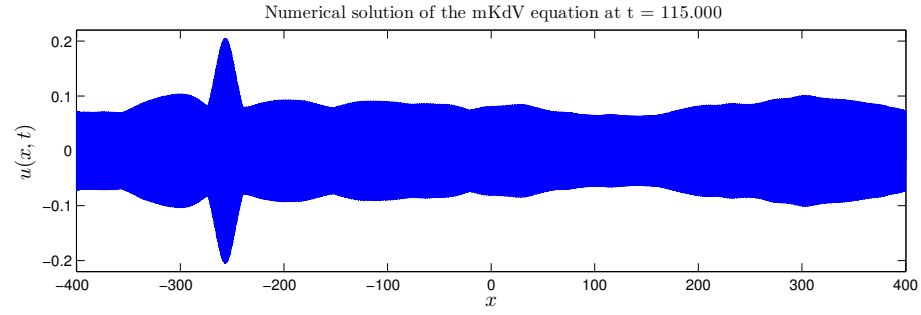

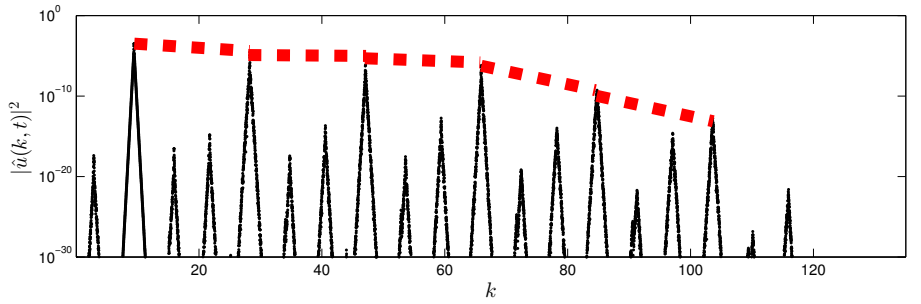

(a) $a = 0.08, t = 115$

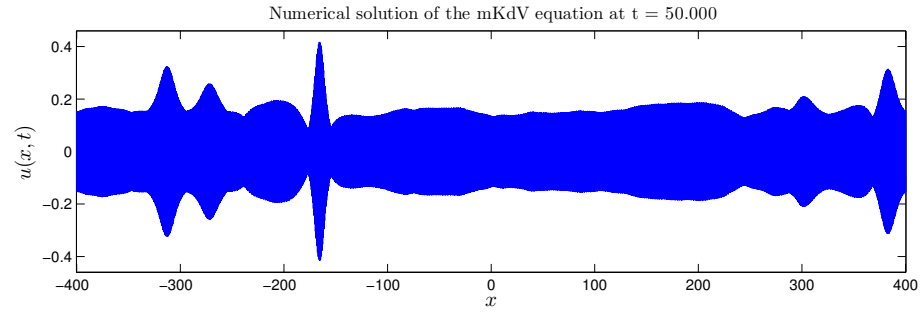

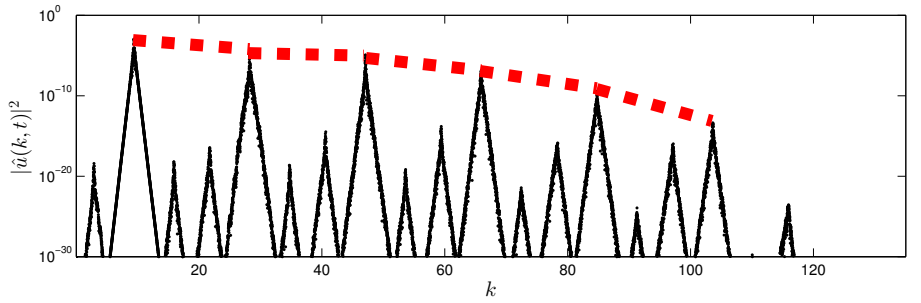

(b) $a = 0.16, t = 50$

Figure 12. *MI simulation for* $k_0 = 5 \times 1.884$*, and two different values of the base wave amplitude* a*. The red bold dotted line corresponds to the energy spectrum shape observed in the numerical simulation.*

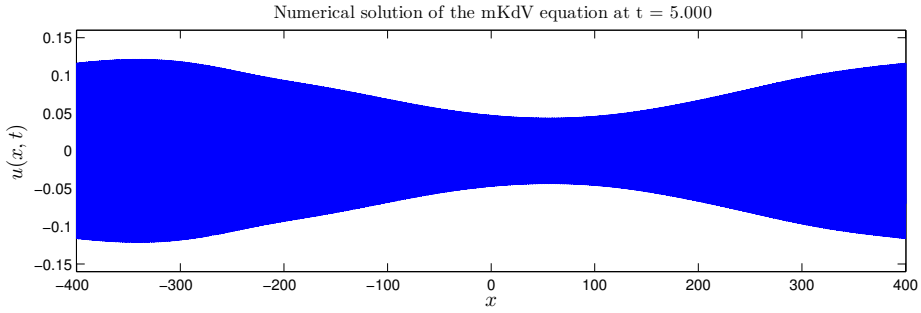

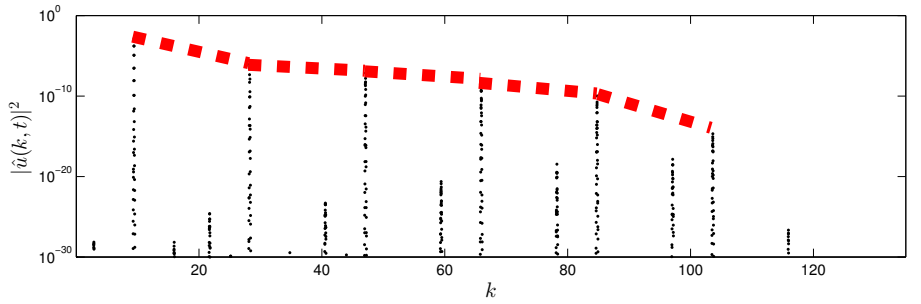

(a) $t = 5$

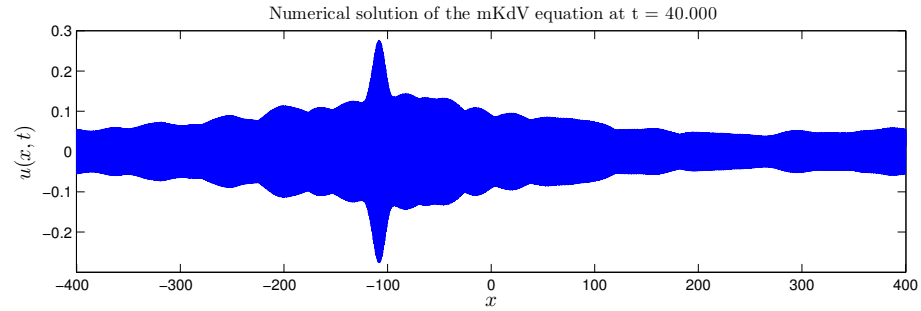

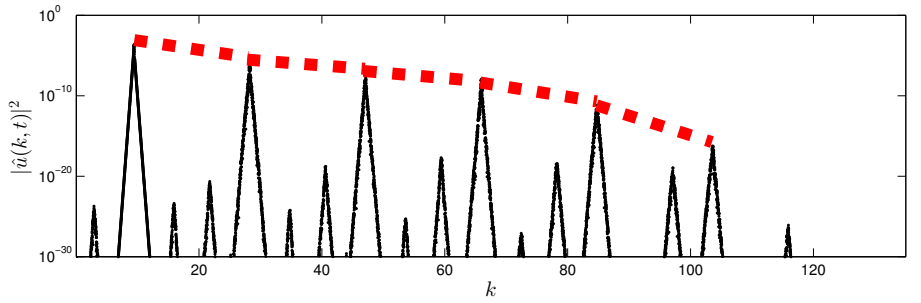

(b) $t = 40$

Figure 13. *MI simulation for* $k_0 = 5 \times 1.884$*, and the perturbation magnitude* $m = 10 \times 0.05 = 0.5$*. The red bold dotted line corresponds to the energy spectrum shape observed in the numerical simulation.*

5.1. Main results

In the numerical experiments we studied the nonlinear stage of the MI evolution aiming to observe the evolution of Fourier spectra additionally to the wave observation in the physical space, already reported in previous studies [16, 36]. The main findings can be briefly summarized in the following list:

- For a wide class of the initial conditions leading to the MI we clearly observe the formation of the direct (*i.e.* in the direction of increasing wavenumbers k) D-cascade. The ranges of parameters considered in this study are given here:
  Amplitude: $a = 0.01 \div 0.24$
  Perturbation magnitude: $m = 0.05 \div 0.5$
  Base wavenumber: $k_0 = 1.8 \div 60.0$
  Simulation time horizon: $T = 40 \div 2000 \propto \mathcal{O}(\varepsilon^{-2})$
  Number of Fourier harmonics: $N = 1024 \div 131\,072$
- In our numerical simulation the MI develops on the dynamical time scales of the order of $\mathcal{O}(\varepsilon^{-2})$ which is in agreement with theoretical predictions [28].
- It is interesting to note that this time scale refers to the complete development of the MI in the physical space (see Figure 9(*d, e*)). On the other hand one can see that the main structure of the D-cascade is already observable in Fourier spectra from the first instances of the dynamical evolution. Consequently, the development of the MI in the physical space corresponds to the spectral broadening of cascading modes. It is remarkable that their positions and energies are quasi-stationary.
- The observed D-cascade skeleton in the Fourier space is very robust and it has the exponential decay $\mathcal{E}_k \propto \exp(-\alpha \cdot k)$ (see Figures 9 and 10). The exponent α was found to be independent of the base wave amplitude a for fixed values of other parameters.
- The increase of k_0 (the base wave wavenumber) has more drastic consequences on the spectrum shape. The agreement with the exponential spectrum $\mathcal{E}_k \propto \exp(-\alpha \cdot k)$ is not satisfactory anymore. This highly nonlinear regime requires a more detailed investigation with higher resolutions in the Fourier space in order to obtain a longer cascade before making some conclusions about its shape (most of simulations presented in this study were already performed with $N = 32\,768$ Fourier harmonics).
- We performed a series of numerical experiments for different values of the perturbation magnitude $m = 0.05 \div 0.5$. We conclude that the main features of the D-cascade described above are preserved (see Figure 13). The choice of the perturbation influences the time scale on which the MI will develop in the physical space. Generally, higher magnitudes of the perturbation tend to accelerate this process.

5.2. Perspectives

5.2.1 Inverse cascade

So far we observed and studied in details the formation and structure of the direct D-cascade. However, the theory predicts the possibility of the inverse D-cascade existence. In future investigations we will study under which conditions the inverse D-cascade can be observed in the mKdV equation.

5.2.2 Modulation of cnoidal waves

The question of modulational stability or instability for periodic traveling waves of the KdV-type with *finite amplitudes* ($a = \mathcal{O}(1)$) has been investigated quite recently in [23, 24, 25, 6]. The authors suggested an elegant way of determining which periodic traveling wave solutions, $u(x,t) = v(x-ct)$, to mKdV are modulationally unstable. Indeed, substitution of $v(x-ct)$ in (1.3) together with simple transformations allows to rewrite (1.3) in the Hamiltonian form as

$$(v')^2 = 2(E - V(v;c,a)) ,$$

where $V(v;c;a) \doteq v^4/4 - cv^2/2 - au$. Here, E is like the ODE Hamiltonian energy, and V is the potential energy. This argument gives you the existence of a three parameter family parameterized by a, E, c of periodic traveling wave solutions to the KdV-type equation. Now the stability of a periodic traveling wave solution of mKdV can be reduced to the properties of the roots of quartic polynomial:

$$P(z) = E - V(z;c,a).$$

If all four roots are real, the solution is stable, otherwise it is unstable, [6]. From this simple characterization, lots of results follow: all cnoidal wave solutions of KdV (corresponding to $a = 0$) are modulationally stable, while all the dnoidal solutions (corresponding to $a = 0$) are modulationally unstable. The above result allows also for $a \neq 0$, and so gives information on solutions which are not simply expressible in terms of Jacobi elliptic functions. It would be interesting to check whether or not the model of D-cascade can be adopted for the case of waves with finite amplitudes. This is the work in progress.

On Figure 14 we show some preliminary results on the numerical simulation of slowly modulated cnoidal waves (1.5) to the mKdV equation. The exact periodic travelling solution was deformed as in the previous sine-wave simulations according to (4.1), with the same value of the parameter δ, and $K_0/k_0 = 120$.

Our computations show that for $s = 0.59$ this polynomial has four complex roots (theory gives no conclusion) and for $s = 0.95$ two real roots (instability). The results of the numerical simulations are shown on Figure 14(a,b) correspondingly. In particular, one can see that for so strong nonlinearities the distance between cascading modes is decreasing as we go further down to the small scales. The question of the strongly nonlinear waves stability remains essentially underinvestigated, especially in the cases where the theory is not conclusive.

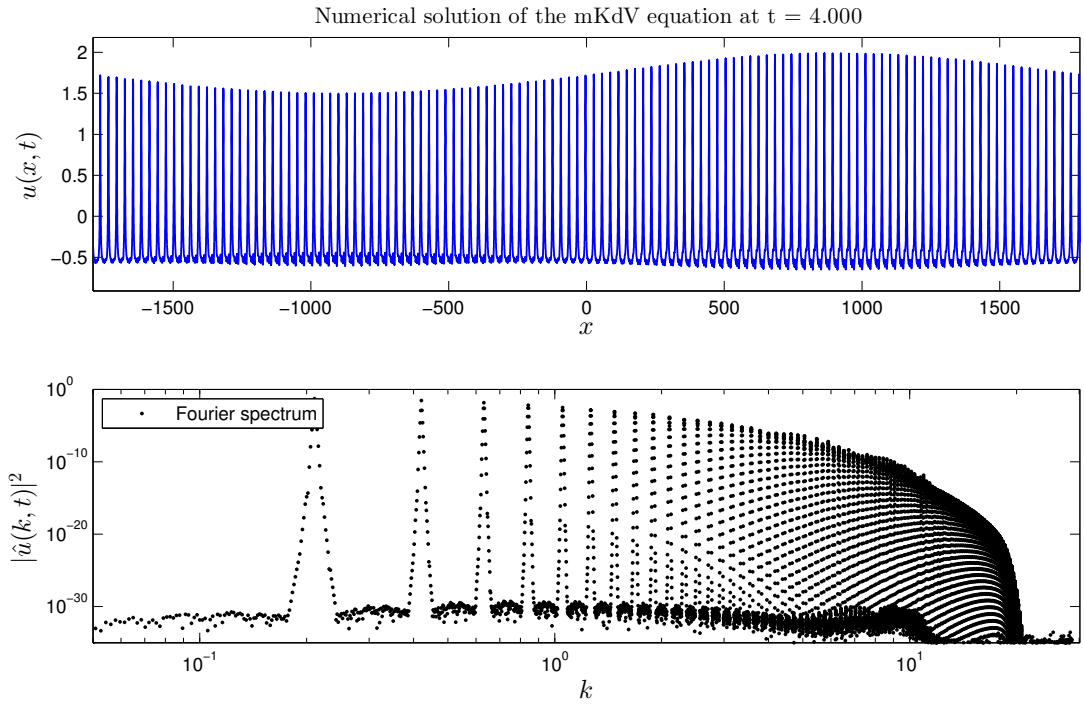

(a) $s = 0.59$

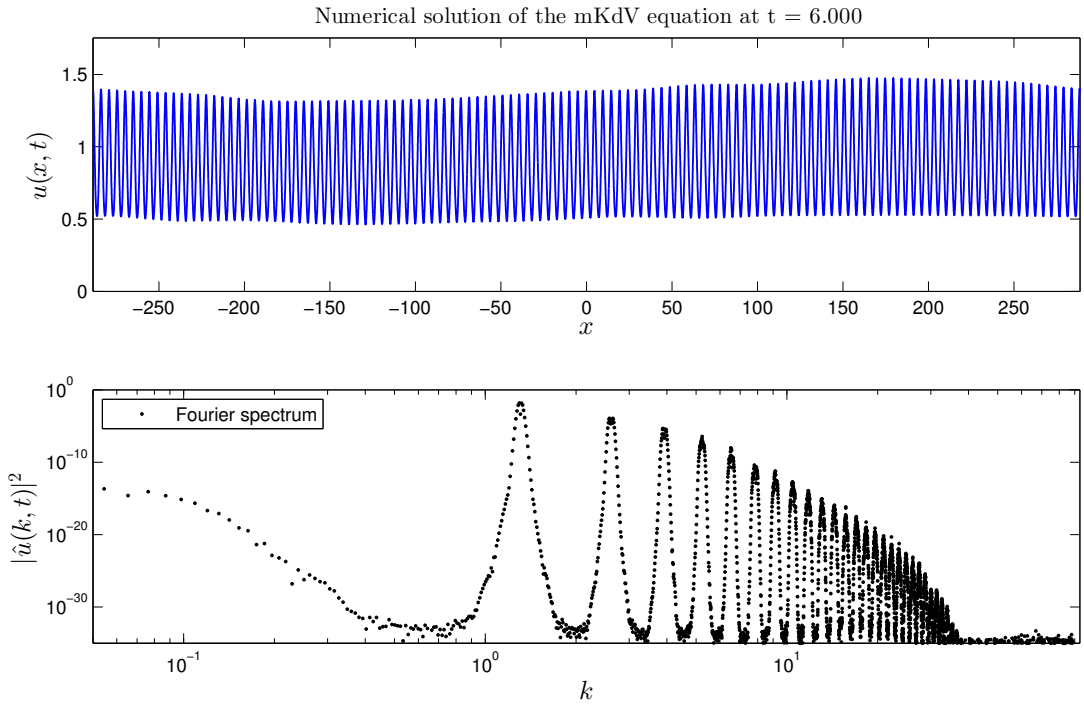

(b) $s = 0.95$

Figure 14. *Example of a large amplitude cnoidal wave simulation with a modulated envelope perturbation.*

Acknowledgments

The authors would like to thank Professors Mat Johnson (University of Kansas) and Fritz Gesztesy (University of Missouri) for interesting discussions and most useful comments. This research has been supported by the Austrian Science Foundation (FWF) under projects P22943-N18 and P24671.

A. Transformations

It is well known that the mKdV equation can be transformed into the classical KdV equation

$$\mathrm{KdV}(v_\pm) \doteq v_t \pm 6vv_x + v_{xxx}$$

by Miura transformation, [30]:

$$\mathrm{KdV}(v_\pm) = (2u \pm \partial_x)\mathrm{mKdV}.$$

As this transformation has the nontrivial kernel, solutions of KdV equation are solutions of the KdV equation but not vice versa. However, a very interesting result by Geszetesy & Holden, [14], can be regarded as a "*partial invertibility*" of the Miura transformation in the following sense. Introducing the first order differential expression

$$\widetilde{P}(V) = 2V\partial_x - V_x.$$

Then one derives

$$\mathrm{mKdV}(\varphi) \doteq \pm\partial_x(\psi^{\pm1}((\psi^{\mp1})_t - \widetilde{P}(V_\pm)\psi^{\mp1})),$$

where

$$\varphi = \psi_x/\psi, \quad \psi > 0, \quad V_\pm = \varphi^2 \pm \varphi_x.$$

Next, let $V = V(x,t)$ be a solution of the KdV equation, $\mathrm{KdV}(V) = 0$, and $\psi > 0$ be function satisfying

$$\psi_t = \widetilde{P}(V)\psi, \quad -\psi_{xx} + V\psi = 0,$$

Then φ solves the KdV equation, $\mathrm{mKdV}(\varphi) = 0$, [14].

References

[1] M. J. Ablowitz and H. Segur. *Solitons and the Inverse Scattering Transform*. Society for Industrial & Applied Mathematics, 1981.

[2] S. Y. Annenkov and V. I. Shrira. Role of non-resonant interactions in the evolution of nonlinear random water wave fields. *J. Fluid Mech.*, 561:181–207, Aug. 2006.

[3] T. B. Benjamin and J. E. Feir. The disintegration of wavetrains in deep water. Part 1. *J. Fluid Mech.*, 27(417), 1967.

[4] V. I. Bespalov and V. I. Talanov. Filamentary Structure of Light Beams in Nonlinear Liquids. *JETP Lett.*, 3:307, 1966.

[5] J. P. Boyd. *Chebyshev and Fourier Spectral Methods*. 2nd edition, 2000.

[6] J. C. Bronski, M. A. Johnson, and T. Kapitula. An index theorem for the stability of periodic travelling waves of Korteweg-de Vries type. *Proc. R. Soc. Edinburgh Sect. A*, 141(06):1141–1173, Nov. 2011.

[7] J. R. Cash and A. H. Karp. A variable order Runge-Kutta method for initial value problems with rapidly varying right-hand sides. *ACM Transactions on Mathematical Software*, 16(3):201–222, Sept. 1990.

[8] P. Denissenko, S. Lukaschuk, and S. Nazarenko. Gravity Wave Turbulence in a Laboratory Flume. *Phys. Rev. Lett.*, 99(1):014501, July 2007.

[9] K. B. Dysthe. Note on a modification to the nonlinear Schrödinger equation for application to deep water. *Proc. R. Soc. Lond. A*, 369:105–114, 1979.

[10] M. Frigo. A fast Fourier transform compiler. In *Proc. 1999 ACM SIGPLAN Conf. on Programming Language Design and Implementation*, volume 34, pages 169–180. ACM, May 1999.

[11] M. Frigo and S. G. Johnson. FFTW: An adaptive software architecture for the FFT. In *Proc. 1998 IEEE Intl. Conf. Acoustics Speech and Signal Processing*, volume 3, pages 1381–1384. IEEE, 1998.

[12] M. Frigo and S. G. Johnson. The Design and Implementation of FFTW3. *Proceedings of the IEEE*, 93(2):216–231, 2005.

[13] U. Frisch. *Turbulence: The Legacy of A. N. Kolmogorov*, volume 317. Cambridge University Press, Cambridge, Apr. 1995.

[14] F. Gesztesy and H. Holden. The Cole-Hopf and Miura transformations revisited. In *Mathematical physics and stochastic analysis. Essays in honor of Ludwig Streit*, pages 198–214. World Scientific, Singapore, 2000.

[15] R. Grimshaw. Internal Solitary Waves. In R. Grimshaw, editor, *Environmental Stratified Flows*, pages 1–27. Springer US, 2002.

[16] R. Grimshaw, D. Pelinovsky, E. Pelinovsky, and T. Talipova. Wave group dynamics in weakly nonlinear long-wave models. *Phys. D*, 159(1-2):35–57, Nov. 2001.

[17] R. Grimshaw, E. Pelinovsky, T. Talipova, M. Ruderman, and R. Erdelyi. Short-Lived Large-Amplitude Pulses in the Nonlinear Long-Wave Model Described by the Modified Korteweg-De Vries Equation. *Stud. Appl. Math.*, 114(2):189–210, Feb. 2005.

[18] E. Hairer and G. Wanner. *Solving Ordinary Differential Equations II. Stiff and Differential-Algebraic Problems*. Springer Series in Computational Mathematics, Vol. 14, 1996.

[19] M. Haragus and T. Kapitula. On the spectra of periodic waves for infinite-dimensional Hamiltonian systems. *Phys. D*, 237(20):2649–2671, Oct. 2008.

[20] K. Hasselmann. On the non-linear energy transfer in a gravity-wave spectrum Part 1. General theory. *J. Fluid Mech.*, 12(04):481–500, Mar. 1962.

[21] S. J. Hogan. The fourth-order evolution equation for deep-water gravity-capillary waves. *Proc. R. Soc. A*, 402(1823):359–372, 1985.

[22] T. Y. Hou and R. Li. Computing nearly singular solutions using pseudo-spectral methods. *J. Comp. Phys.*, 226(1):379–397, Sept. 2007.

[23] M. A. Johnson. Stability of Small Periodic Waves in Fractional KdV-Type Equations. *SIAM J. Math. Anal.*, 45(5):3168–3193, Oct. 2013.

[24] M. A. Johnson and K. Zumbrun. Rigorous Justification of the Whitham Modulation Equations for the Generalized Korteweg-de Vries Equation. *Stud. Appl. Math.*, 125(1):69–89, Mar. 2010.

[25] M. A. Johnson, K. Zumbrun, and J. C. Bronski. On the modulation equations and stability of periodic generalized Korteweg-de Vries waves via Bloch decompositions. *Phys. D*, 239(23-24):2057–2065, Nov. 2010.

[26] E. Kartashova. Energy spectra of 2D gravity and capillary waves with narrow frequency band excitation. *EPL*, 97(3):30004, Feb. 2012.

[27] E. Kartashova. Energy transport in weakly nonlinear wave systems with narrow frequency band excitation. *Phys. Rev. E*, 86(4):041129, Oct. 2012.

[28] E. Kartashova. Time scales and structures of wave interaction exemplified with water waves. *EPL*, 102(4):44005, May 2013.

[29] A. N. Kolmogorov. The Local Structure of Turbulence in Incompressible Viscous Fluid for Very Large Reynolds Numbers. *Proc. R. Soc. Lond. A*, 434(1890):9–13, July 1991.

[30] R. M. Miura. Korteweg-de Vries Equation and Generalizations. I. A Remarkable Explicit Nonlinear Transformation. *J. Math. Phys.*, 9(8):1202, 1968.

[31] R. M. Miura, C. S. Gardner, and M. D. Kruskal. Korteweg-de Vries Equation and Generalizations. II. Existence of Conservation Laws and Constants of Motion. *Journal of Mathematical Physics*, 9(8):1204, 1968.

[32] A. C. Newell and B. Rumpf. Wave Turbulence. *Ann. Rev. Fluid Mech.*, 43(1):59–78, Jan. 2011.

[33] H. Ono. Algebraic Soliton of the Modified Korteweg-de Vries Equation. *J. Phys. Soc. Jpn.*, 41(5):1817–1818, Nov. 1976.

[34] E. J. Parkes. The modulation of weakly non-linear dispersive waves near the marginal state of instability. *J. Phys. A: Math. Gen.*, 20(8):2025–2036, June 1987.

[35] S. B. Pope. *Turbulent Flows*, volume 1. Cambridge University Press, Cambridge, Jan. 2000.

[36] M. S. Ruderman, T. Talipova, and E. Pelinovsky. Dynamics of modulationally unstable ion-acoustic wavepackets in plasmas with negative ions. *J. Plasma Phys.*, 74(05), Apr. 2008.

[37] E. Tobisch. Energy spectrum of ensemble of weakly nonlinear gravity-capillary waves on a fluid surface. *Accepted to JETP Lett.*, 2014.

[38] L. N. Trefethen. *Spectral methods in MatLab*. Society for Industrial and Applied Mathematics, Philadelphia, PA, USA, 2000.

[39] M. P. Tulin and T. Waseda. Laboratory observations of wave group evolution, including breaking effects. *J. Fluid Mech.*, 378:197–232, Jan. 1999.

[40] G. B. Whitham. Variational Methods and Applications to Water Waves. *Proc. R. Soc. Lond. A*, 299(1456):6–25, June 1967.

[41] H. Xia, M. Shats, and H. Punzmann. Modulation instability and capillary wave turbulence. *EPL*, 91(1):14002, July 2010.

[42] H. C. Yuen and B. M. Lake. Nonlinear dynamics of deep-water gravity waves. *Adv. App. Mech.*, 22:67–229, 1982.

[43] V. E. Zakharov and N. N. Filonenko. Weak turbulence of capillary waves. *Journal of Applied Mechanics and Technical Physics*, 8(5):37–40, 1971.

[44] V. E. Zakharov, V. S. Lvov, and G. Falkovich. *Kolmogorov Spectra of Turbulence I*. Series in Nonlinear Dynamics, Springer-Verlag, Berlin, 1992.

[45] V. E. Zakharov and L. A. Ostrovsky. Modulation instability: The beginning. *Phys. D*, 238(5):540–548, Mar. 2009.

LAMA, UMR 5127 CNRS, Université de Savoie, Campus Scientifique, 73376 Le Bourget-du-Lac Cedex, France
E-mail address: Denys.Dutykh@univ-savoie.fr
URL: http://www.denys-dutykh.com/

Institute for Analysis, Johannes Kepler University, Linz, Austria
E-mail address: Elena.Tobisch@jku.at
URL: http://www.dynamics-approx.jku.at/lena/